Coupled Mode Approach to the Analysis of Thin Film S0 Lamb wave Resonators

V. Yantchev*, L. Arapan and I. Katardjiev
Dept. Solid State Electronics, Uppsala University, Box 534, 751 21 Uppsala, Sweden
E-mail: veya@angstrom.uu.se , URL: http://hermes.teknikum.uu.se/~veya/

***Abstract*—In this work the applicability of the Couplings-of-Modes (COM) approach to the analysis of one- and two- port thin AlN film plate acoustic resonators (FPAR), utilizing the S0 Lamb wave, is discussed. Analysis based on the Fluquet-Bloch theorem as well as COM parameter extraction from a micromachined FPAR test structure are simultaneously used to verify the applicability of the COM approach. Subsequently, COM based design of 2-port FPARs for use in feed back loop oscillators and cascaded filters is demonstrated. The proposed theoretical approach can easily be adapted to the case of S0 Lamb wave resonators utilizing reflections from suspended membrane edges.**

I. Introduction

During the last five years, a new class of thin film microacoustic devices, based on the utilization of lateral plate guided waves, is being developed. Plate guided waves in thin films have been traditionally observed as a spurious and degrading content in the response of thin film bulk acoustic resonators (FBARs). Among the variety of plate modes observed, the lowest order symmetric Lamb wave (S0) has attracted special attention due to its weak dispersion, acoustic velocity in excess of 10 000 m/s [1] and moderate electromechanical coupling (up to 3 – 3.5 %) [2, 3]. Two distinct approaches to the design of S0 Lamb wave resonators are being simultaneously and independently developed. The first one is based on the utilization of Lamb wave reflections from the free edges of a suspended membrane [4-6] (Contour Extensional Mode Resonators), [7] (Thin Film Piezoelectric on Silicon Resonators), while the other is based on the utilization of Lamb wave reflections from periodic gratings on the thin film membrane [1,8,9] (Thin Film Plate Acoustic Resonators (FPARs)). In this work FPARs utilizing distributed reflectors are studied. Their micro-fabrication has been previously presented [9] and is not further considered inhere.

Historically, FPARs are being developed since 2003 and the first prove of principle results have been submitted for publication in the late 2004 [8]. Later, theoretical studies on the S0 Lamb wave propagation characteristic [10] enabled the design of efficient reflecting gratings bringing substantial improvements to the device response [9]. Further studies on the factors limiting the FPARs performance led to the development of FPARs exhibiting Qxf=2.8 10^{12} at a frequency of around 850 MHz. Subsequently, the first 50 Ohm matched two-port FPAR configurations have been designed, having a loaded Q in the range of 1000 with insertion losses of about -5dB [11]. Quite recently, temperature compensated FPARs utilizing composite AlN/SiO2 membranes, have demonstrated a second order temperature coefficient of frequency β=-31 ppb/K^2, while preserving the electromechanical coupling and the device performance [12].

The above described results reveal to a certain extent the potential and the physical limitations of the FPAR technology, but its full capabilities are yet to be realized. Thus, the development of FPAR analytical and design tools appear to be a quite natural continuation of the FPAR research. In this work the applicability of the Coupling-of-Modes (COM) analysis towards the design of FPARs is discussed.

II. The Coupling-of-Modes (COM) Analysis

The propagation characteristics of the lowest order symmetric Lamb wave under periodical gratings indicated the existence of a quite well pronounced stopband behavior. The experimental results demonstrated so far are in an excellent agreement with the theoretical predictions [10] and provide the opportunity to analyze the device performance in a very similar manner to their well-known surface acoustic wave (SAW) counterparts. Further, the excitation of the mode mimicks the geometries used in SAW resonant structures, which in turn justifies the use of the well established SAW formalisms for the analysis of the FPAR performance. Most generally, plate wave devices can be simulated by the use of a specifically modified SAW analysis technique based on the FEM/BEM approach in combination with the periodical Green's function formalism [13]. This SAW analysis technique has been developed just during the last decade due to its technical complexity and computer power requirements. Inhere, we discuss the applicability of the much more robust Couplings-of-Modes (COM) approach to the analysis and simulation of one- and two- port FPARs. Most generally COM is a phenomenological model for guided wave propagation and excitation, which is widely employed for the design of high-performance, SAW devices. The analysis based

The Work is supported by the Vinnova WISENET Center of Excellence and Göran Gustafsson Stiftelse

on the COM model gives very simple and analytical solutions with a surprisingly good accuracy provided the COM parameters are properly determined. The COM equations and parameters used inhere are thoroughly derived and discussed elsewhere [14]. For brevity of the discussion, we reproduce here the list of COM parameters [14], to be considered:

• $k_P = -k_{21} \cdot \lambda_0$ —dimensionless reflectivity per finger pair, where k_{21} is the COM reflectivity parameter and λ_0 is the IDT period;

• V_{S0} – S0 Lamb wave phase velocity in AlN at center frequency $f_0 = V_{S0} / \lambda_0$;

• αn —normalized COM transduction coefficient,

$$\alpha n = \frac{\alpha \cdot \lambda_0}{\sqrt{W / \lambda_0}}$$

where W is the device aperture, and α is the COM transduction coefficient;

• $\gamma_P = \gamma \cdot \lambda_0$ – attenuation per wavelength [Np/λ];

• D — dimensionless velocity dispersion, which is empirically extracted from:

$$(f - f_0) / f_0 = (1 - D) \cdot (k - k_0) / k_0 ,$$

where $D = 1 - V_{GR} / V_{S0}$ and $V_{GR} = \partial\omega / \partial k$ is the Lamb wave group velocity;

• Cn —Normalized Capacitance (per IDT pair, per unit aperture) [F/m].

Initially, the COM analysis is employed for the extraction of the COM parameters of a 12μm wavelength synchronous one-port FPAR (see fig.1) fabricated onto a 2 μm thick highly c-textured AlN membrane as presented by its frequency response in figure 2 (the solid line). The experimental curve (solid line) in Fig. 2 is fitted according to the COM model until a best fit is obtained (dashed line). As seen, the simulated curve reproduces fairly well the experimental response. Only the peak to the right of the main resonance appeared slightly overestimated due to higher order degradation effects not accounted in this analysis.

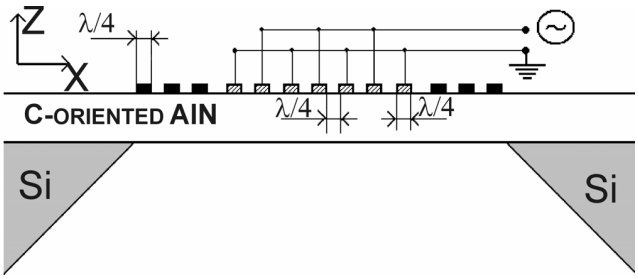

Figure 1. Schematic view of one-port FPAR

Table I shows the values of the COM parameters extracted from the fitting procedure in Fig. 1. To further verify the applicability of the COM approach, the extracted parameters are compared to the theoretical predictions in the next section.

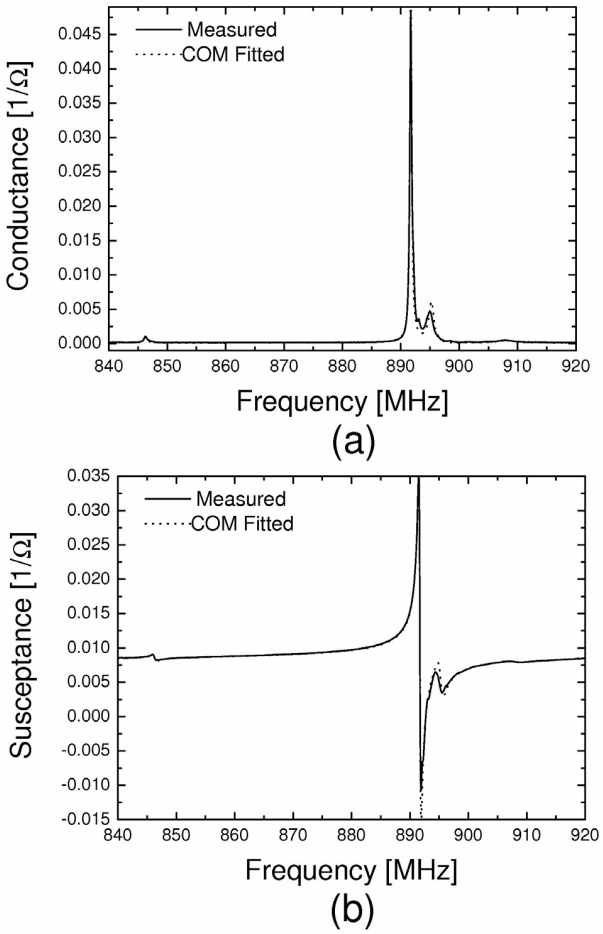

Figure 2. Measured vs COM-fitted admittance a) Conductance b) Susceptance

TABLE I. VALUES OF THE EXTRACTED COM PARAMETERS

Layout: 2μm thick c-AlN, 270nm thick Al electrodes, λ_0=12μm	
COM Parameters:	Value
S0 Velocity (V_{S0} [m/s])	10435.05
Velocity Dispersion (D)	$3.5 \cdot 10^{-2}$
Normalized Reflection Coefficient (k_P)	$16.5 \cdot 10^{-2}$
Normalized Capacitance (Cn [pF/m])	81.9
Normalized Transduction Coefficient (αn [$\Omega^{-1/2}$])	$13.3 \cdot 10^{-5}$
Intrinsic Attenuation (γ_P [Np/λ])	$9.48 \cdot 10^{-4}$
Parasitic Electrical Resistance (R_S [Ω])	1.81

III. COM PARAMETERS: THEORY VS EXTRACTION

A. Propagation characteristics

The extracted central velocity of the S0 mode is 10435 m/s which is in a close agreement with the experimentally measured value from a splitted electrode transducer [9] and

represents a value slightly higher than the theoretically predicted V_{S0}=9850 m/s from the bulk AlN material constants. The velocity dispersion was found to be close to the extracted value, D=0.025, assuming continuous mass loading by means of the Adler's approach [15]. The propagation characteristics of Lamb waves in periodical strip gratings are determined by the presence of a frequency stopband with an upper stopband edge relatively insensitive to electrode thickness variations [10]. It has been shown elsewhere [14] that the frequency positions of the stop band edges can be used for the estimation of the reflection |χ12| coupling-of-modes (COM) parameter

$$|k_{21}| = \frac{f_U - f_L}{f_U + f_L} k_0 , \qquad (1)$$

where f_U and f_L are the frequencies of the upper and lower stopband edges, respectively and $k_0 = 2\pi/\lambda_0$ is the wavenumber at resonance frequency. Accordingly, the Floquet theorem based harmonic analysis [10] can be employed for the determination of the normalized reflection coefficient. Note that in this case the charge distribution is neglected, due of the leading role of the mechanical perturbations. This approximation is sufficient to analyze the basic trends. It is further noted that the difference between the single crystalline materials constants and the actual thin film constants (as evident from the difference between the theoretically calculated and the experimentally measured central velocity of the Lamb wave) further limits the accuracy of this calculation. In figure 3, the normalized reflection coefficient is shown as a function of the strip thickness for a given plate thickness to wavelength ratio.

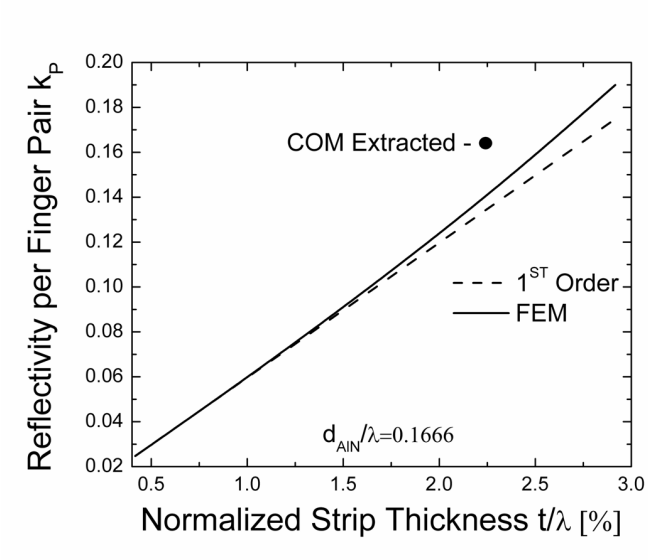

Figure 3. Reflectivity per finger pair

The results obtained through the Floquet-Bloch analysis to the first order of approximation (assuming constant particle displacement throughout the strips) are first compared to the results obtained from a FEM based analysis using COMSOL, where the upper and the lower stopband edges are identified by using eigen-frequency analysis of single wavelength plate section with applied periodic boundary conditions. Note the deviation from the linear behavior predicted through the first-order Datta-Hussinger boundary conditions applied within the Floquet-Bloch anlysis. The latter represent the uncertainty of the first-order boundary conditions applied. In fact, the grating strips represent an important part of the waveguide due the small plate thickness to wavelength ratio. The accuracy of the model can be further improved by considering higher order terms in the mechanical boundary conditions. The extracted COM reflection coefficient is slightly larger than the theoretically predicted, which is thought to emanate from the above mentioned difference between the materials constant of the thin AlN film and the bulk AlN substrate.

In figure 4 the specific waveguiding at the upper and lower stopband edge is shown, respectively. Note the excellent agreement between the Fluquet-Bloch based analysis and the FEM simulation. At the upper stopband edge where synchronous FPARs operate, the energy distribution is symmetric with respect to the plate median plane, while at the lower stopband edge energy trapping towards the periodic grating is observed.

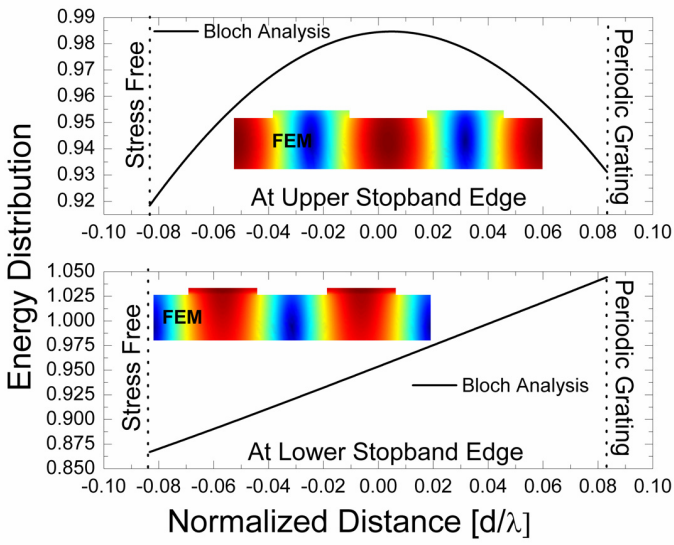

Figure 4. Disperssive Waveguiding

B. *Static Capacitance*

For the determination of the normalized capacitance Bløtekjær's method [16] for analyzing structures consisting of metal strips in dispersive media is used. In this formalism the tangential component of the electric field and the surface charge distribution are represented by an infinite sum of harmonics:

$$E_x = \sum_{n=-\infty}^{\infty} A_n e^{-j(s+n)\theta} , \sigma = j \sum_{n=-\infty}^{\infty} A_n \varepsilon_n S_n e^{-j(s+n)\theta} , \qquad (2)$$

where $s = k\Lambda/(2\pi)$, $\theta = 2\pi x/\Lambda$, S_n=sgn(n), k-is the wavenumber, Λ is the transducer pitch and

$\varepsilon_n = \varepsilon_S(k + 2n\pi/\Lambda)$ is the effective static permittivity (zero acoustic wave velocity) of the n-th Floquet-Bloch harmonic. The constants *An* are determined according to the requirement for zero charge at the electrode free surface and zero tangential electric field at the electrodes. Using some mathematical identities for the Legendere polynomials the electric field and charge density are found:

$$E_x = -j\frac{\theta}{|\theta|}\frac{\sqrt{2}e^{-j\theta s}e^{j\theta/2}}{\sqrt{\cos(\Delta)-\cos(\theta)}}\sum_m \psi_m e^{-jm\theta} \qquad (3)$$

for $\Delta < |\theta| < \pi$ and $E_x = 0$ for $|\theta| < \Delta$,

$$\sigma = j\frac{\sqrt{2}e^{-j\theta s}e^{j\theta/2}\varepsilon_\infty}{\sqrt{\cos(\theta)-\cos(\Delta)}}\sum_m \psi_m e^{-jm\theta} \qquad (4)$$

for $|\theta| < \Delta$ and $\sigma = 0$ for $\Delta < |\theta| < \pi$.

Here $\Delta = \pi a/\Lambda$ (a – strip width) and each constant A_n can be uniquely defined by a linear combination of ψ_m. For brevity further details will be omitted. Following this approach the normalized capacitance is determined from the admittance of a transducer pair. In figure 5, the normalized capacitances calculated for two major types of IDT transducers are shown respectively. The first type is a regular IDT, while the second type is an IDT over a floating bottom electrode. The agreement between the COM-extracted and theoretically predicted values is excellent as seen from Fig. 5.

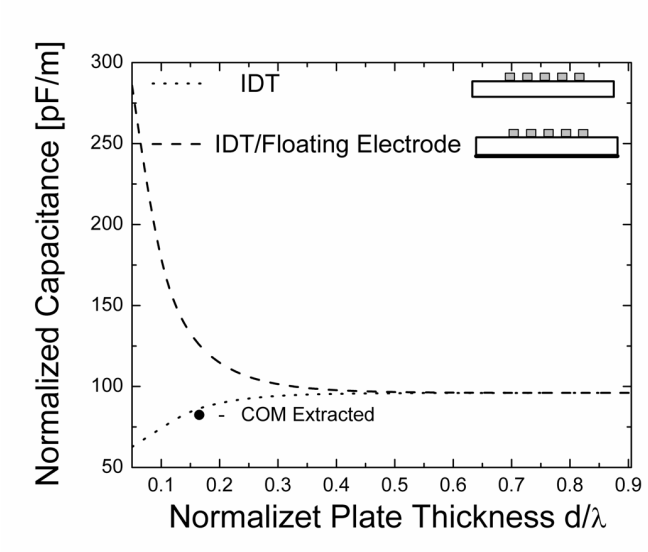

Figure 5. Normalized Capacitance Cn vs plate thickness to wavelenght ratio

C. COM Transduction

The transduction coefficient is directly related to the magnitude of waves generated by a transducer pair under a unit drive voltage. It depends both on the intrinsic electromechanical coupling and the single element charge, responsible for the Lamb wave excitation. The Bløtekjær's formalism can be further extended towards the calculation of the single element charge distribution $\overline{\sigma}_{1e}(k) = \int_0^1 \overline{\sigma}(k,s)ds$, where $\overline{\sigma}(k,s) = \int_{-\infty}^{\infty} \sigma e^{jkx} dx$ is the Fourier transformation of the spatial charge distribution σ. Applying the quasi-static approximation, the acoustic conductance $G_a(\omega_0)$ per IDT pair, at center frequency can be calculated and subsequently the normalized COM transduction coefficient αn determined. In a quasi-static approximation, the acoustic conductance is defined as [17]

$$G_a(\omega_0) = \omega_0 W \Gamma_s |\overline{\sigma}_{1e}(k_f)|^2 . \qquad (5)$$

The latter is a function of the single element charge distribution $\overline{\sigma}_{1e}(k_f)$, the acoustic wave number at open circuited surface conditions k_f, the IDT aperture W and the Lamb wave term of the Green's function $G_{Lamb} = j\Gamma_s \exp(-jk|x|)$, presented in Ingebrigsren's approximation as $\Gamma_S = k_{Lamb}^2/(2\varepsilon_S(k_f))$, where $k_{Lamb}^2 = 2(V_{OC} - V_{SC})/V_{OC}$ is the intrinsic Lamb wave electromechanical coupling, and V_{OC} and V_{SC} are the Lamb wave velocities at electrically free and metalized plate surface, respectively [2, 17].

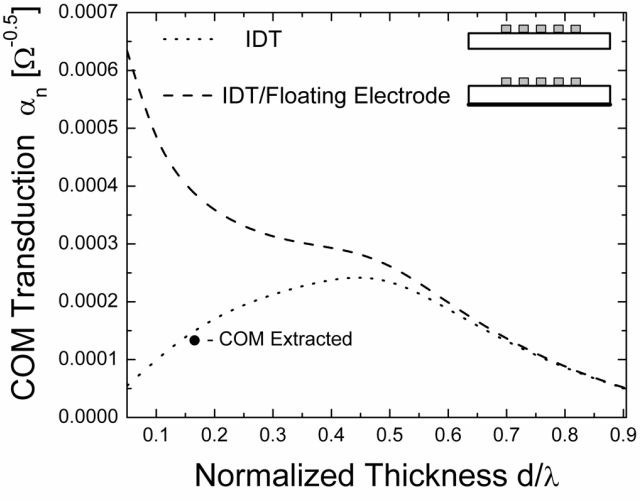

Figure 6. Normalized COM transduction vs palte thickness to wavelenght ratio

In figure 6, the normalized COM transduction coefficients calculated for two major types of transducers are shown. The agreement between the COM-extracted and the theoretically predicted values is excellent. Evidently, the IDT/Floating electrode transducer offers a much higher transduction

coefficient at relatively small plate thickness to wavelength ratios.

IV. COM Analysis of 2-port Lamb Wave Resonators

In this section, the applicability of the COM approach to the analysis of 2-port FPARs is demonstrated. In figure 7a,b a comparison between measured and COM-predicted response of a synchronous 2-port FPAR is shown. The measured response shown in Fig.7a corresponds to a device with 43 strips in the IDT and 48 strips in the reflectors, a cavity length $L=7.5\lambda_0$ and an aperture of $50\lambda_0$.

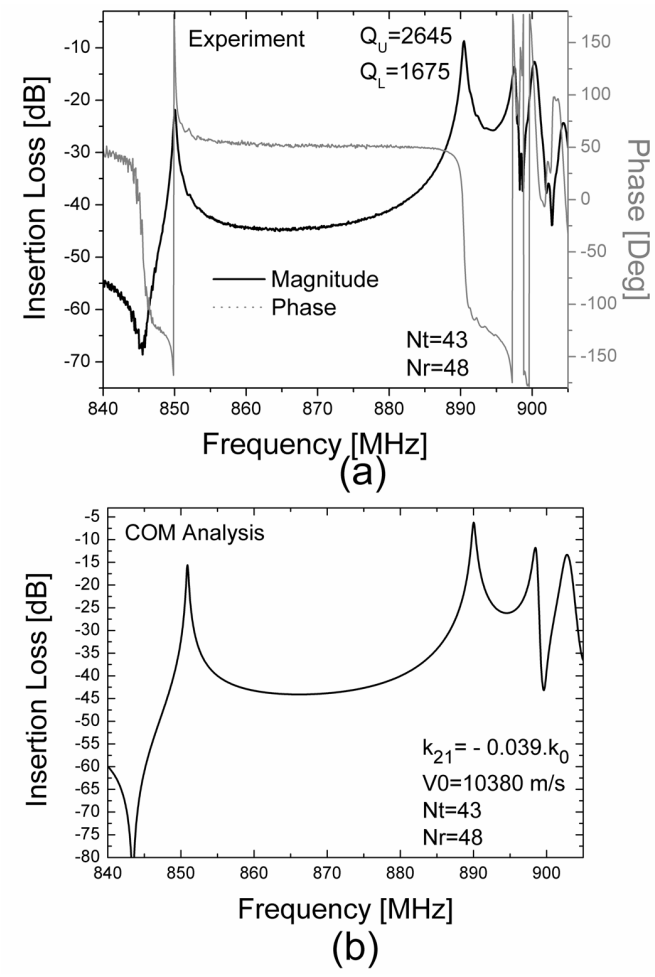

Figure 7. Measured Frequency Respnce vs COM predicted of a 2 Port synchronous FPAR configuration

In figure 8 a comparison between the measured and COM-predicted response of an asynchronous 2-port FPAR is shown. The response shown in Fig.8a corresponds to a device with 41 strips in the IDT and 52 strips in the reflectors, a cavity length $L=1.125\lambda_0$ and an aperture of $50\lambda_0$.

In both cases the agreement between theory and experiment is very good. To further improve the accuracy of the model, dispersive reflection coefficient should be introduced to take into account the dispersion of the waveguiding (see figure 4).

It is noted that the theoretical considerations regarding the determination of the COM parameters do not take into account technology induced variations in the thin film material constants. Therefore, the parameters theoretically obtained should be considered as approximate. The accuracy can be improved if for a given technology and layer thickness the COM parameters are extracted from test structures and subsequently applied to the design of more complicated resonator/filter topologies.

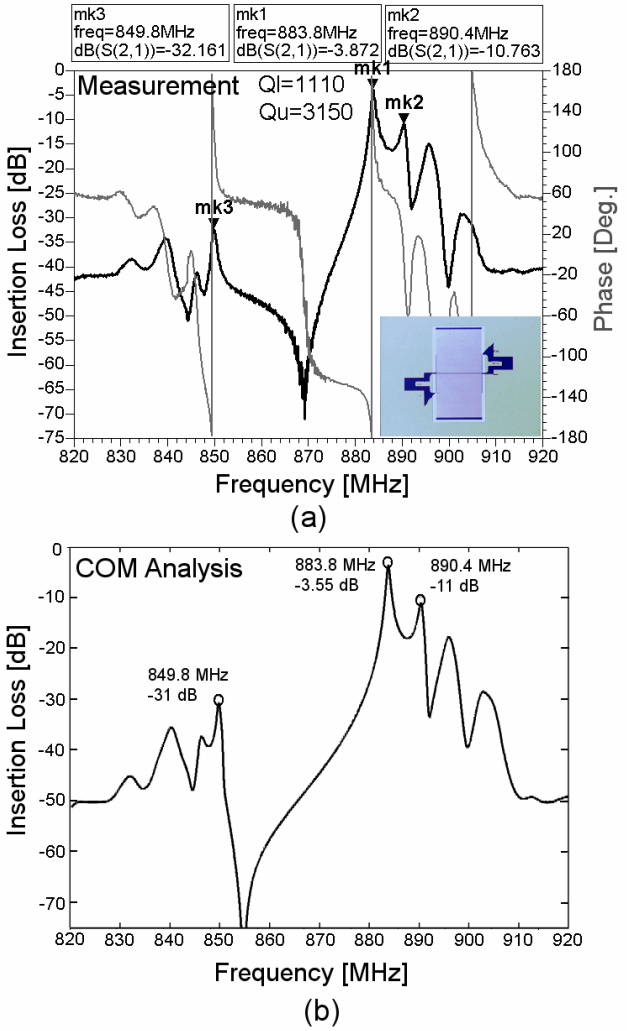

Figure 8. Measured Frequency Respnce vs COM predicted of a 2 Port asynchronous FPAR configuration

V. Conclusions

The Coupling-of-Modes Approach has been thoroughly investigated as a means for the analysis and design of thin film plate acoustic resonators (FPARs). A close agreement between theory and experiment has been demonstrated, justifying thus the applicability of the formalism. The method thus developed is expected to facilitated the design of FPARs that meet narrow specifications. It is further noted the ability to extend the method towards the analysis of RF contour-extensional mode resonators utilizing multi-wavelength transducers and free edge reflections (an alternative approach has been

recently presented [18]). In such structures the periodic transducer can be nalyzed through the presented COM routine including charge distribution and propagation effects, while the reflection from the suspended membrane edges can be defined by their amplitude and phase.

REFERENCES

[1] J. Bjurström, V. Yantchev, and I. Katardjiev, "Thin film Lamb wave resonant structures," The first approach," Solid State Electron., vol. 50, pp. 322–326, 2006

[2] V. Yantchev and I. Katardjiev, "Quasi-static transduction of the fundamental symmetric Lamb mode in longitudinal wave transducers," Appl. Phys. Lett., vol. 88, pp. 214101–214103, 2006.

[3] M. Benetti, D. Cannatà, F. Di Pietrantonio, E. Verona, "Guided Lamb Waves in AlN Free Strips", Proc. Ultras. Symp. 2007, pp. 1673-1676.

[4] P. J. Stephanou and A P. Pisano, "GHZ Contour Extensional Mode Aluminum Nitride MEMS Resonators", Proc. IEEE Ultrason. Symp. 2006, pp. 2401-2404.

[5] G. Piazza, P. J. Stephanou, and A. P. Pisano, "Piezoelectric Aluminum Nitride Vibrating Contour-Mode MEMS Resonators," J. Microelectromech. Syst., vol. 15, no. 6, pp. 1406–1418, Dec. 2006.

[6] M. Desvergne, E. Defaÿ, D. Wolozan, M. Aid, A. Volatier, Y. Deval and J.-B. Bégueret, "Intermediate Frequency Lamb Wave Coupled Resonator Filters for RF Receiver Architectures", 37th European Solid State Device Research Conference, 2007, pp. 358 – 361.

[7] R Abdolvand, H. Lavasani , G. Ho, F. Ayazi , "Thin-film piezoelectric-on-silicon resonators for high-frequency reference oscillator applications," IEEE Trans. Ultrason. Ferroelectr. Freq. Control, Vol. 55, pp. 2596–2606, 2008

[8] J. Bjurström, I. Katardjiev, and V. Yantchev, "Lateral-fieldexcited thin-film Lamb wave resonator," Appl. Phys. Lett., vol. 86, pp. 154103–154106, 2005.

[9] V. Yantchev and I. Katardjiev, "Micromachined Thin Film Plate Acoustic Resonators Utilizing the Lowest Order Symmetric Lamb Wave Mode", IEEE Trans. Ultrason., Ferroelect., Freq. Contr., vol. 54, no. 1, 2007, pp. 87-95.

[10] V. Yantchev and I. Katardjiev, "Propagation characteristics of the fundamental symmetric Lamb wave in thin aluminum nitride membranes with infinite gratings," J. Appl. Phys., vol. 98, pp. 849101–849107, Oct. 2005.

[11] V. Yantchev and I. Katardjiev, "Thin AlN film resonators utilizing the lowest order symmetric Lamb mode: further developments," Proc. 2007 IEEE Int. Freq. Contr. Symp., pp 1067–1072, 2007

[12] G. Wingqvist, L. Arapan, V. Yantchev and I. Katardjiev, "A micromachined thermally compensated thin film Lamb wave resonator for frequency control and sensing applications," J. Micromech. Microeng., Vol. 19, 035018, 2009

[13] T. Pastureaud, W. Daniau, V. Laude, M. Wilm, Y. Malecamp, and S. Ballandras, "Characterization and prediction of transverse plate resonators built using mixed strip and groove gratings," in Proc. IEEE Ultrason. Symp., 2001, pp. 93–96.

[14] V. Plessky and J. Koskela, in Advances in Surface Acoustic Wave Technology, Systems and Applications. vol. 2, pp. 1– 82, Singapore: World Scientific Publ., 2001.

[15] A. A. Nassar and E. L. Adler, "Propagation and Electromechanical Coupling to Plate Modes in Piezoelectric Composite Membranes", Proc. Ultras. Symp., pp. 369-372, 1983.

[16] K. Bløtekjær, K. Ingebrigsten and H. Skeie, "A Method for Analyzing Waves in Structures Consisiting of Metal Strips on Dispersive Media," IEEE Trans. Electron. Dev., Vol. ED-20, No. 12, pp. 1133-1138, 1973

[17] D. Morgan, Surface-Wave Devices for Signal Processing,Amsterdam: Elsevier, 1991, pp.47 -100.

[18] Jan Kuypers and Albert Pisano, "Green's Function Analysis of Lamb Wave Resonators", Proc. 2008 IEEE Int. Ultrason. Symp., pp. 1548-1551, 2008